Effect of Positional Substitution on the Optical Response of Symmetrically Disubstituted Azobenzene Derivatives

A. A. Blevins and G. J. Blanchard*

Department of Chemistry, Michigan State University, East Lansing, Michigan 48824-1322

Received: November 11, 2003; In Final Form: February 10, 2004

We have synthesized a series of symmetrically substituted *p*-diamidoazobenzenes, and we compare their steady-state and time-resolved responses to those of *p*-diaminoazobenzene and azobenzene. Our experimental and computational data indicate that the identity of the azobenzene ring substituent plays a significant role in determining the ordering of excited electronic states and the oscillator strengths for the various $S_n \leftarrow S_0$ transitions. We find experimentally that the symmetric disubstitution of azobenzenes also influences the S_0 isomerization surface, with the largest S_0 barrier being found for the unsubstituted compound and the smallest barrier for *p*-diaminoazobenzene. We understand these data in the context of the relative electron-donating character of the para side groups.

Introduction

Azobenzenes are a family of compounds that has found wide use because of their facile photoisomerization and relatively high barrier to thermal (ground state) isomerization. These properties are of potential utility in the development of molecular-scale information storage and optical switching strategies.[1−11] Among the key issues under investigation for the azobenzenes is the ability of substitution about their aromatic rings to mediate their optical properties and isomerization behavior. While it is typically assumed that the linear optical response and isomerization behavior of these chromophores are linked, this relationship has not been established. The purpose of this work is to examine how the presence of substituents on the azobenzene phenyl rings influences the spectroscopic and isomerization behavior of these compounds. We have synthesized a family of symmetrically para-disubstituted azobenzenes and have studied their steady-state optical properties. We have also evaluated the branching ratio for isomerization and the rate of trans isomer recovery for these species. Our findings indicate that the addition of substituents to the azobenzene chromophore can influence the steady-state and time-resolved optical properties of the chromophore significantly, and the isomerization surfaces for these molecules are affected as well. This is not a surprising result because of the relationship between electronic structure and state ordering and the electron density distribution for the bond(s) that dominate the isomerization coordinate. We understand this finding in the context of the N═N bond dominating the isomerization behavior of these molecules, and the effective bond order of this moiety is influenced by the presence of electron-donating or electron-withdrawing substituents on the phenyl rings. Our finding that the isomerization barrier is reduced when electron-donating substituents are placed on the rings indicates that it is the π^* state that is influenced most strongly, and these findings are supported by the steady-state spectra. Our data also point to the potential importance of asymmetric substitution of the azobenzene rings in structurally mediating isomerization.[12]

* To whom correspondence should be addressed. E-mail: blanchard@chemistry.msu.edu.

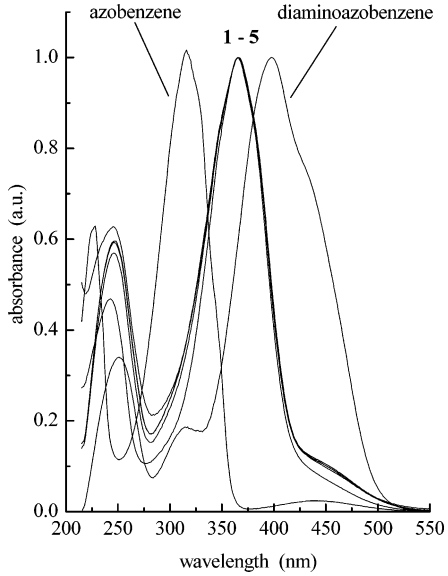

Figure 1. Normalized absorption spectra of azobenzene, *p*-diaminoazobenzene, and the series of *p*-diamidoazobenzenes **1**−**5**, as indicated. Molar absorptivities of these compounds are given in Table 1.

Experimental Section

Steady-State Absorption Spectroscopy. The absorbance spectra of the various azobenzenes reported here were obtained on a Varian/Cary model 300 UV/vis absorption spectrometer. Spectral resolution for all measurements was 1 nm, and the normalized absorption spectra are shown in Figure 1. The molar absorptivities and absorption maxima of the compounds are given in Table 1.

Calculated Results. Semiempirical calculations were performed on a Windows-based PC using Hyperchem v. 6.0. Dihedral angles were incremented for isomerization barrier calculations using macros written in Excel.[21] For these calculations, initial geometry optimization was performed using PM3 parametrization, and then single point calculations were made for the molecule at each incremented angle without additional geometry optimization.

10.1021/jp037436w CCC: $27.50
Published on Web 03/25/2004

TABLE 1: Absorption Maxima and Molar Absorptivities of of Azobenzene, *p*-Diaminoazobenzene, and the *p*-Diamidoazobenzenes 1−5

compound	absorption max (nm)	ϵ_{max} (L/(mol cm))	ϵ_{450} (L/(mol cm))
azobenzene	313	22 400	500
p-diaminoazobenzene	394	27 800	1630
1	364	17 900	1300
2	364	23 750	2400
3	364	24 200	2530
4	364	24 900	2500
5	364	25 300	2450

Chemical Synthesis and Sample Preparation. The series of *p*-diamidoazobenzenes we report on here were synthesized using a modification of a standard polyamido polymerization route.[13] We have replaced the dicarboxylic acid with an acid chloride, precluding the possibility of polymerization and eliminating the need for an initiator. The reaction is illustrated in Scheme 1. 4,4′-Azodianiline was purchased from Sigma-Aldrich (CAS 538-41-0). The reactions were carried out under an inert atmosphere to limit hydrolysis of the acid chloride. Methylene chloride, acetone, and tetrahydrofuran were purchased from Sigma-Aldrich and used as received. *N*-Methylmorpholine was used to scavenge hydrochloric acid produced during the reaction. Reaction times of 30 min at room temperature were typical, with little or no increase in yield for longer reaction times. Typical reaction conditions were for 2 mmol of 4,4′-azodianiline to be combined with 8 mmol of *N*-methylmorpholine and 8 mmol of the appropriate acid chloride in 150 mL of CH_2Cl_2. Following completion of the reaction, the solution was washed with 150 mL of 2 M HCl. The diamidoazobenzene precipitated from solution and was collected by filtration. The resulting solid was dissolved in acetone and washed with an equal volume of brine solution to separate the derivatized azobenzene from the acid reaction byproducts, and the crude product was then separated from the acetone. The solid was purified by recrystallization from methanol/water (80:20). As the alkyl substituent of the acid chloride increased in length, the purity of the *p*-diamidoazobenzene product could be increased significantly by additional washing with brine solution. The reaction to synthesize **5** produced lower yields due to the nonpolar nature of the product. For this reaction THF was used in place of CH_2Cl_2 as the solvent due to the limited solubility of nonanoyl chloride in CH_2Cl_2. The use of THF as the solvent required a methanol washing of the recovered solid to remove unreacted starting materials but eliminated the need for recrystallization.

SCHEME 1: (top) Structures of Compounds Investigated in This Work; (bottom) Reaction Scheme for Synthesis of *p*-Diamidoazobenzenes[a]

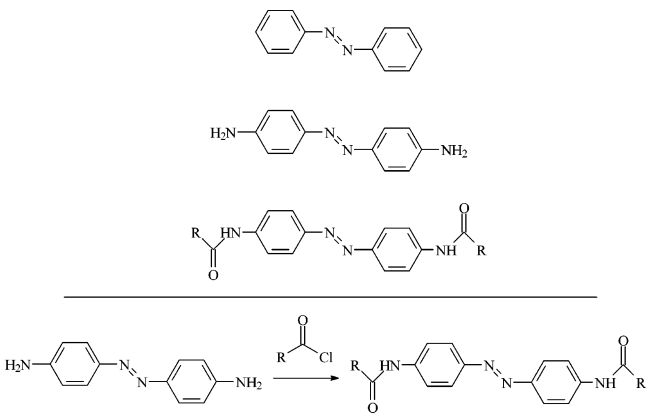

[a] **1**: R = $-CH_3$; **2**: R = $-CH_2CH_3$; **3**: R = $-(CH_2)_2CH_3$; **4**: R = $-(CH_2)_3CH_3$; **5**: R = $-(CH_2)_7CH_3$.

Compound 1 (*N*-[4-(4-(Acetylamino)phenylazo)phenyl]-acetamide). This compound was produced with a crude yield of 80% and recrystallized yield of 53% using CH_2Cl_2 solvent. The resulting brown flakes showed proton NMR peaks (300 MHz, *d*-methanol) at δ 2.14 ppm (s, 6H alkyl protons), 7.70 ppm (m, 4H on benzene ring), and 7.90 ppm (m, 4H on benzene ring). The mass spectrum (GC/MS) of the compound showed peaks at *m*/*z* 43, 65, 92, 134, 162, and 296.

Compound 2 (*N*-[4-(4-(Propionylamino)phenylazo)phenyl]-propionamide). This compound was produced with a crude yield of 73% and recrystallized yield of 54% using CH_2Cl_2 solvent. The resulting brown flakes showed proton NMR peaks (300 MHz, *d*-methanol) at δ 1.22 ppm (m, 6H β to carbonyl), 2.44 ppm (m, 4H α to carbonyl), 7.77 ppm (m, 4H on benzene ring), and 7.87 ppm (m, 4H on benzene ring). The mass spectrum (GC/MS) of the compound showed peaks at *m*/*z* 57, 92, 119, 148, 149, 176, 324, and 325.

Compound 3 (*N*-[4-(4-(Butyrylamino)phenylazo)phenyl]-butyramide). This compound was produced with a crude yield of 46% and recrystallized yield of 44% using CH_2Cl_2 solvent. The resulting orange needles showed proton NMR peaks (300 MHz, *d*-methanol) at δ 0.92 ppm (m, 6H γ to carbonyl), 1.63 ppm (m, 4H β to carbonyl), 2.29 ppm (m, 4H α to carbonyl), 7.70 ppm (m, 4H on benzene ring), and 7.90 ppm (m, 4H on benzene ring). The mass spectrum (GC/MS) of the compound showed peaks at *m*/*z* 43, 71, 92, 120, 162, 190, 211, 282, 352, and 353.

Compound 4 (Pentanoic Acid [4-(4-(Pentanoylamino)-phenylazo)phenyl]amide). This compound was produced with a crude yield of 34% and recrystallized yield of 30% using CH_2Cl_2 solvent. The resulting orange powder showed proton NMR peaks (300 MHz, *d*-methanol) at δ 0.89 ppm (m, 6H δ to carbonyl), 1.32 ppm (m, 4H γ to carbonyl), 1.61 ppm (m, 4H β to carbonyl), 2.33 ppm (m, 4H α to carbonyl), 7.67 ppm (m, 4H on benzene ring), and 7.78 ppm (m, 4H on benzene ring). The mass spectrum (GC/MS) of the compound showed peaks at *m*/*z* 57, 92, 120, 176, 211, 296, 380, and 381.

Compound 5 (Nonanoic Acid [4-(4-(Nonanoylamino)-phenylazo)phenyl]amide). This compound was produced with a crude yield of 69% using THF solvent, and no recrystallization was performed. The resulting yellow powder showed proton NMR peaks (300 MHz, *d*-dimethyl sulfoxide) at δ 0.85 ppm (d, 6H), 1.25 ppm (m; 20H η, ϕ, ϵ, δ, and γ to carbonyl), 1.55 ppm (m, 4H β to carbonyl), 2.33 ppm (m, 4H α to carbonyl), 6.81 ppm (d, 4H on benzene ring), 7.52 ppm (d, 4H on benzene ring), and 7.81 ppm (s, amide proton). The mass spectrum (GC/MS) of the compound showed peaks at *m*/*z* 43, 108, 120, 211, 232, 352, 490, and 492.

Results and Discussion

The azobenzenes find significant use in work aimed at optical information storage and switching because of their somewhat unusual isomerization properties. Until recently, the standard picture for the isomerization of azobenzenes was that there is a significant barrier to isomerization in the S_0 state, with the magnitude of the barrier being a consequence of the azo (N═N) moiety. We are not aware of an accurate determination of the thermal isomerization barrier for azobenzenes, either experimental or computational, but it has been thought to be on the order of 50−60 kcal/mol. Because of this substantial energy, the modeling of this barrier cannot be done using the usual

assumption of a one-dimensional isomerization coordinate; i.e., both isomerization and ring rotation must be coordinated in some unresolved manner. When excited to the S_1 state, the azobenzene chromophore is thought to isomerize by an inversion, or rehybridization mechanism, and excitation to the S_2 state is thought to cause isomerization to proceed by rotation about the azo bond, which is taken to be substantially single bond in character.[14] This widely accepted picture has continued to stir debate, owing to the relative time scales of large-amplitude molecular motion and internal conversion from the S_2 to the S_1 manifold.

Recent elegant work by both the Tahara[14] and Kobayashi[15] groups has cast doubt on the "standard" picture. Using femtosecond optical techniques, Tahara's group has shown that excitation to the S_2 state of azobenzene undergoes rapid relaxation to the S_1 state, where isomerization proceeds.[14] When viewed in the context of the characteristically short lifetime of higher excited electronic states in organic molecules, and the time frame required for inertial motion of the phenyl ring(s), these results are fully consistent with the behavior of most organic chromophores. The Kobayashi group, using chirped femtosecond pulses, has demonstrated clearly that vibronic coupling is substantial in an excited azobenzene derivative and that the redistribution of energy within the vibrational manifold of the S_1 state serves to mediate the isomerization behavior of that species.[15] These findings on the earliest stages of relaxation within azobenzenes not only shed significant light on the factors mediating isomerization but also underscore the fact that a full understanding of isomerization in azobenzenes remains to be achieved.

With this background, we consider whether it is possible to mediate the isomerization behavior of azobenzenes by synthetic means. We are interested in being able to incorporate para-disubstituted azobenzenes into layered assemblies for the purposes of probing local structure using isomerization and for determining whether a layered structural motif is capable of storing information via optical read/write means. In an attempt to address these issues, we have focused on the synthesis and characterization of a family of simple para-disubstituted azobenzenes, with particular interest in the influence of the para disubstitution on the spectroscopic and isomerization behavior of the resulting chromophores. The compounds studied are structurally simplified models for disubstituted species capable of layer incorporation. We consider the experimental spectroscopic and calculated isomerization results separately.

Steady-State Spectroscopy. The steady-state absorption spectroscopy of azobenzene is well understood. The $S_1 \leftarrow S_0$ transitions for both the trans and cis forms are characterized by weak absorption bands ($\epsilon \sim 500$ L/(mol cm) for cis, $\epsilon \sim 2000$ L/(mol cm) for trans), and these bands are centered at ~434 nm. The $S_2 \leftarrow S_0$ absorption bands for both isomers are stronger, with the trans band at 313 nm ($\epsilon \sim 22\,400$ L/(mol cm)) and the cis band at 254 nm ($\epsilon \sim 12\,000$ L/(mol cm)).[16−18] The addition of amino groups at the para positions causes a substantial change in the absorption spectrum. For *p*-diaminoazobenzene, the dominant absorption band is at ~420 nm ($\epsilon = 22\,800$ L/(mol cm)), with weaker bands seen at 310 and 250 nm. For the solution phase spectra we recorded, we did not attempt to isolate cis and trans conformers, so it is not clear on the basis of the experimental data whether the bands at 310 and 250 nm correspond to trans and cis forms, respectively, or whether these represent two different excited electronic states of the same (presumably trans) conformer. This remarkable change in the absorption spectra resulting from para disubstitution reflects a change in the electronic excited state(s), and this is seen in the results of semiempirical calculations for both cis and trans conformers (Figure 2), where the dominant absorption transition ($S_2 \leftarrow S_0$) is seen to red-shift by ~7000 cm^{-1} upon addition of the *p*-amino functionalities. Reaction of the diamino functionalities to produce the *p*-diamido azobenzene derivatives produces a blue-shifted absorption band relative to the *p*-diamino compound. The experimental spectra can be reconciled with the results of semiempirical calculations for both conformers (Figure 2), and for all of the azobenzenes, it appears that multiple $S_n \leftarrow S_0$ transitions contribute significantly to the observed linear optical response. While the spectral red-shift seen for diamidoazobenzenes relative to that seen for diaminoazobenzenes may appear to violate one's intuition, we believe that these findings are the result of changes in transition oscillator strength of low-lying transitions with the addition of amido substituents rather than actual band shifts. Both experimental data and semiempirical calculations point to the significant substituent dependence of the electronic state energies of the azobenzenes.

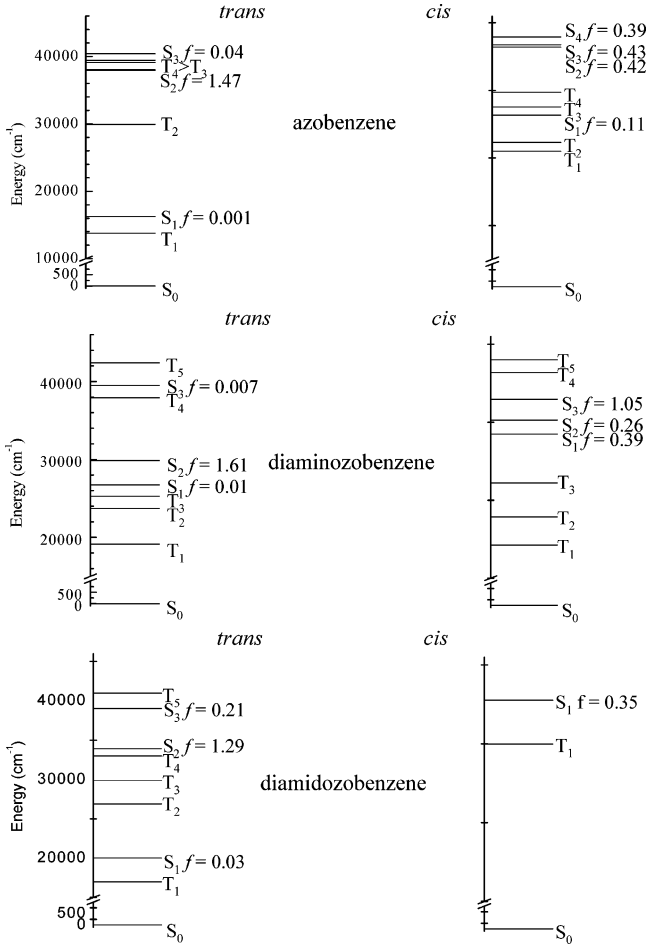

Figure 2. Calculated electronic state energies and oscillator strengths for trans (l) and cis (r) azobenzene (top), trans (l) and cis (r) *p*-diaminoazobenzene (center), and trans (l) and cis (r) *p*-diamidoazobenzene (bottom). Calculations were performed using the PM3 parametrization for geometry-optimized ground-state structures.

The azobenzene derivatives we study here exhibit remarkable substituent-dependent variation in their steady-state optical responses, and these findings are mirrored by substantial changes in the electronic state energies and singlet transition oscillator strengths calculated at the semiempirical level. It appears, on the basis of a comparison of experimental and calculated results for these compounds, that the transition energies are predicted relatively well, but the oscillator strengths for these transitions

are not. Given these findings, intuition may suggest that the isomerization behavior of these molecules would likewise vary with substitution, and we examine this issue next.

To understand the isomerization behavior of azobenzene and the symmetrically disubstituted azobenzenes, we have evaluated the branching ratio for isomer formation and the recovery time required for the samples to return to an equilibrium ground-state population distribution. The branching ratio data are reflective of the location of the ground-state surface maximum and the excited electronic state surface minimum. If these two electronic state features coexist at the same point in conformational space, we would expect a branching ratio of 1; i.e., 50% of the excited molecules relax to form a S_0 trans conformer, and 50% relax to form a S_0 cis conformer. Deviations from this ideal behavior are indicative of either a noncorrespondence between the electronic state surface minima and maxima or a ground-state potential energy surface that is not well characterized in the context of Rulliere's model.[19]

To characterize the branching ratio, we irradiate a sample until the ratio of trans to cis remains constant, as measured by absorption spectroscopy. Because the extinction coefficients of the cis and trans bands will, in general, differ, we need to correct the data either through band ratio measurements or by direct conversion of the absorbance data to concentration data using Beer's law. Upon UV irradiation, the ratio of trans to cis conformers reaches a steady state, which recovers to the equilibrium ratio once UV irradiation of the sample is stopped. The steady-state [trans]/[cis] ratio, prior to recovery, is 0.19 for azobenzene, 0.51 for diamidoazobenzene, and 4.5 for diaminoazobenzene. We note the similarity of azobenzene and diamidobenzene and the contrasting behavior of diaminoazobenzene.

Of perhaps greater significance than the branching ratio data are those for the isomerization recovery. We have measured the isomerization recovery time constants for azobenzene, *p*-diaminoazobenzene, and *p*-diamidoazobenzene. The time constants are for cis → trans conversion and vary enormously with substitution and scale qualitatively with the energy of the dominant electronic transition of the chromophores. For azobenzene, we find that the recovery time after photoisomerization is 10 900 min (Figure 3a), for the *p*-diamidoazobenzenes, the recovery time is 317 min (Figure 3c), and for *p*-diaminoazobenzene, the recovery time is 4.7 min (Figure 3b). These remarkably different time constants for trans recovery are due to variations in the isomerization barrier height, which are related to the electron density distribution about the azo bonds in these compounds. While the back-isomerization time constants are remarkably different for these compounds, it is important to keep in mind that there is a logarithmic relationship between the measured time constant and the barrier height. We have calculated the barrier heights consistent with the experimental back-isomerization data for the substituted azobenzenes, assuming a prefactor for the activated process of 10^{13} Hz.[20] For *p*-diaminoazobenzene, with a characteristic recovery time constant of 4.7 min, we calculate a barrier height of 21.2 kcal/mol, for *p*-diamidoazobenzene, with a recovery time constant of 317 min, we calculate a barrier height of 23.7 kcal/mol, and for azobenzene, with a recovery time constant of 10 900 min, we calculate a barrier height of 25.8 kcal/mol. These barrier heights for S_0 cis → trans back-conversion vary substantially less than the recovery time data would seem to imply, owing to the logarithmic relationship between the recovery rate constant and the barrier height. These results are in qualitative agreement with semiempirical calculations (vide infra).

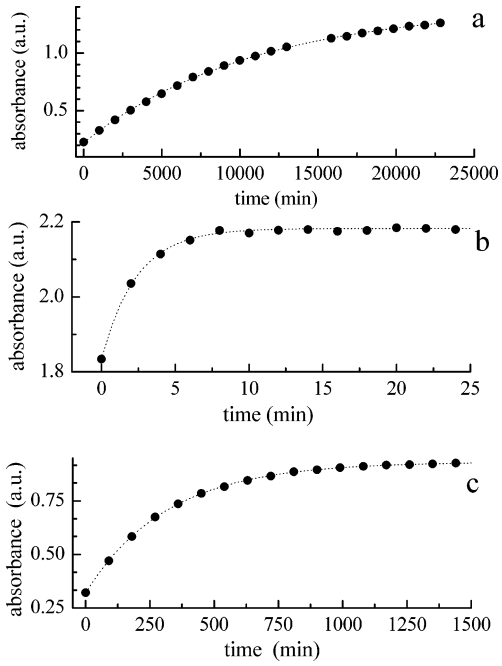

Figure 3. (a) Time-resolved cis → trans absorbance recovery of azobenzene following photoisomerization. The time constant for the recovery is $\tau = 10\,900 \pm 150$ min. (b) Time-resolved cis → trans absorbance recovery of *p*-diaminoazobenzene following photoisomerization. The time constant for the recovery is $\tau = 4.7 \pm 0.6$ min. (c) Time-resolved cis → trans absorbance recovery of *p*-diamidoazobenzene following photoisomerization. The time constant for the recovery is $\tau = 317 \pm 2$ min.

We note that there is an inverse correlation between barrier height and electron donor strength of the para substituents. This correlation is the result of an effective increase in the average electron density of the π^* (antibonding) state, reducing the effective bond order of the N═N bond and thereby reducing the isomerization barrier height. We seek to understand the detailed basis for this relationship and find that the linear optical response of these compounds is useful for this purpose. The ground state (thermal) barrier for isomerization is correlated with the transition cross section of the first allowed electronic transition for these azobenzenes. All of the azobenzenes studied here have transitions in the 400−450 nm region (Figure 1), so it is not the *energy* of the $S_1 \leftarrow S_0$ transition that is related to the thermal back-isomerization barrier height. Rather, it is the transition cross section of the lowest energy transition that is correlated with the barrier height. We rationalize this relationship by noting that a transition cross section is reflective of large overlap integrals for the transitions. The isomerization barrier height is related to the bond order of the N═N bond, and the $S_1 \leftarrow S_0$ transition coordinate is thought to lie along the long axis of the azobenzene molecule. We postulate that the isomerization and electronic transition coordinates are nearly the same. The ground electronic states (HOMOs) of the azobenzenes are characterized by a relatively high bond order of ∼2 for the N═N bond. The first excited singlet states (LUMOs) of these compounds are characterized by a substantial reduction in electron density and thus bond order on excitation. Because the activation barrier for ground-state back-isomerization of the azobenzenes involves a high-energy intermediate state, mixing with states in the S_1 manifold is possible, and the strength of this coupling is reflected in the transition cross sections of the $S_1 \leftarrow S_0$ transitions for both the cis and trans forms. Thus, the more strongly allowed the $S_1 \leftarrow S_0$ transition

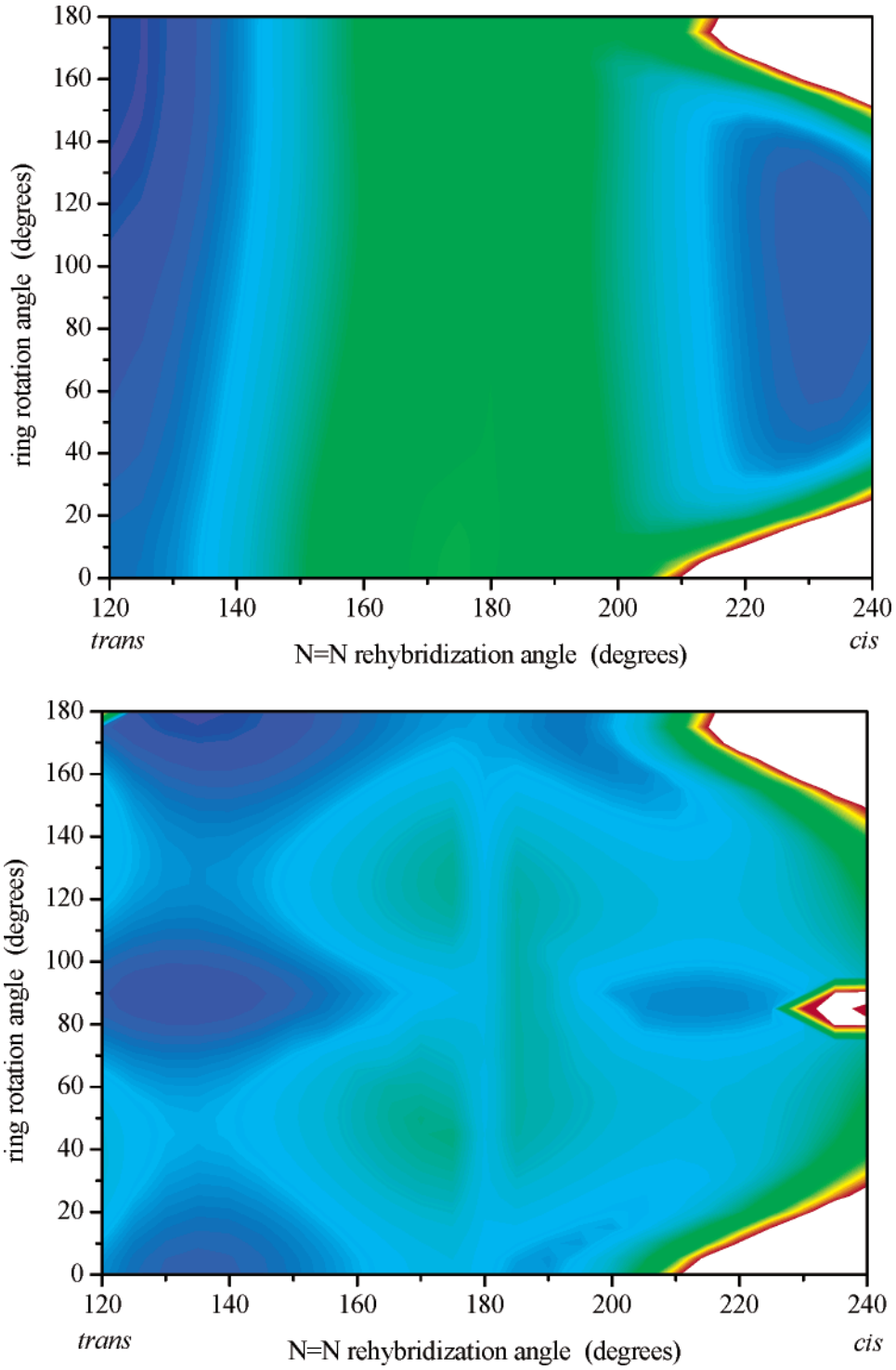

Figure 4. Calculated isomerization surfaces for azobenzene isomerization by rehybridization of an azo nitrogen (*x*-axis) as a function of ring rotation angle (*y*-axis). Top pane is the S_0 surface, and bottom pane is the S_1 surface. Color scale spans 70 kcal/mol.

(Table 1), the more single-bond character there will be for the transition state on the S_0 back-isomerization surface, giving rise to a lower barrier height. This explanation provides qualitative agreement with the experimental data and does not invoke coupling of higher excited electronic states.

We can also understand these data in the context of simple resonance structure arguments. The unique behavior and low back-isomerization barrier of 4,4′-diaminoazobenzene can be accounted for in terms of contributions from the several resonance structures possessing a N−N bond (Scheme 2). Such resonance structures are stabilized by the presence of the electron-donating amine groups at the para positions. For 4,4′-diamidoazobenzene, the groups at the para positions are electron-withdrawing, and the lone pair of the amido nitrogen will interact most strongly with the carbonyl moiety, allowing contributions from zwitterionic species (Scheme 2 bottom, structure ii), precluding significant contributions from structures iii and iv. The result of the presence of the amido groups is that the azo N═N moiety will have substantially more double-bond character than is seen for diaminoazobenzene. On the basis of these qualitative arguments, we expect diaminoazobenzene to have the lowest thermal isomerization barrier, azobenzene the highest,

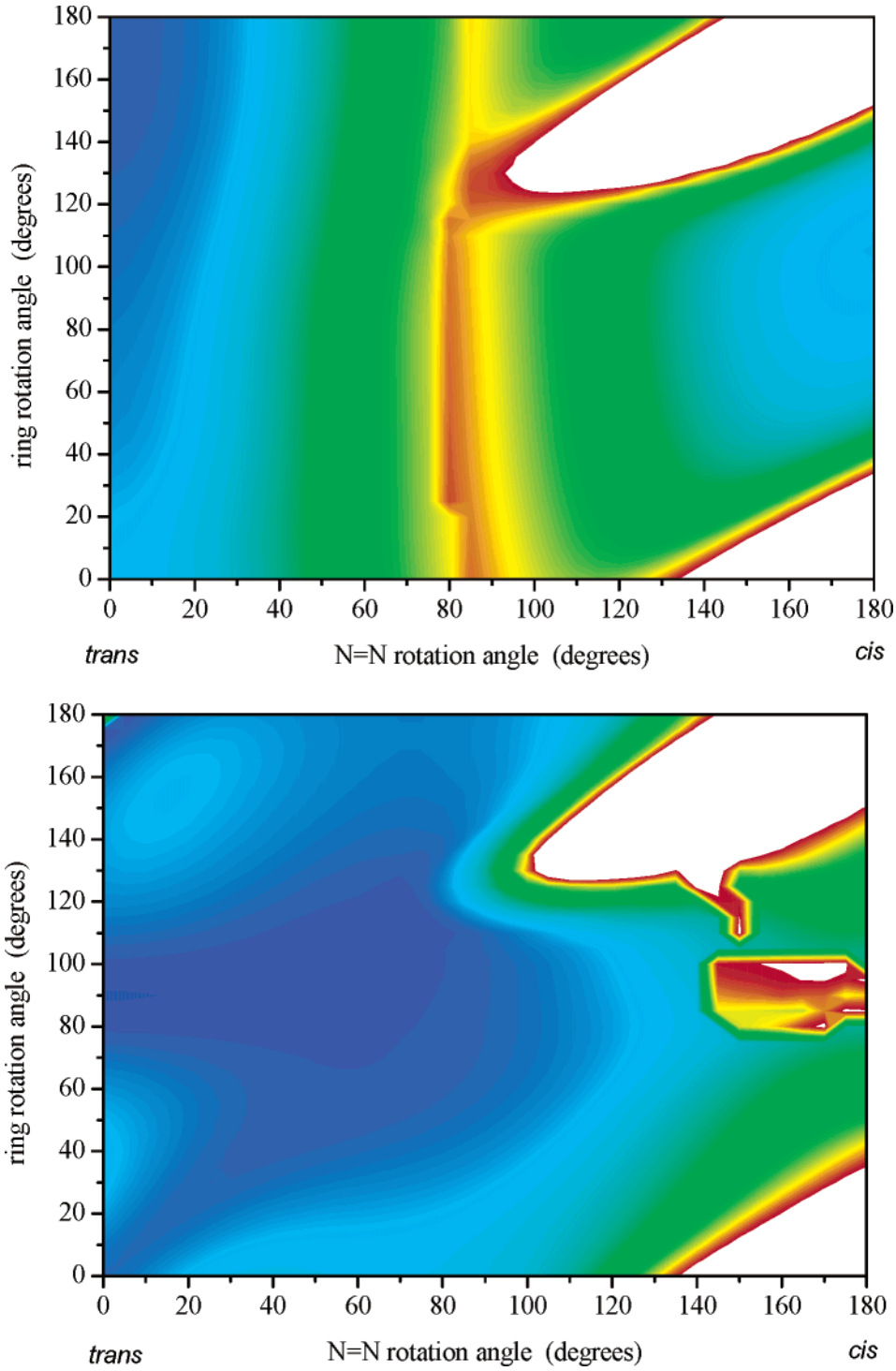

Figure 5. Calculated isomerization surfaces for azobenzene isomerization by rotation of the azo N═N bond (*x*-axis) as a function of ring rotation angle (*y*-axis). Top pane is the S_0 surface, and bottom pane is the S_1 surface. Color scale spans 70 kcal/mol.

and diamidoazobenzene to be intermediate, in agreement with our experimental findings.

We have attempted the calculation of the isomerization surfaces for the substituted azobenzenes, and we find that semiempirical calculations do not reflect the experimental substituent dependence on back-isomerization barrier height. This is not surprising given the parametrization used in semiempirical calculations and the multidimensional nature of the isomerization coordinate for azobenzenes. Even with the limitations of such calculations, we can extract useful information from them. One issue that has not been addressed is the mechanism of ground-state (thermal) isomerization for this class of molecules. Our calculations for azobenzene, presented in Figures 4 and 5, show the calculated energy surfaces for the S_0 (a) and S_1 (b) states, for isomerization by rehybridization of one N (Figure 4) or rotation about the N═N bond (Figure 5). These calculated results predict that (thermal) isomerization in the ground state proceeds by rehybridization and not by −N═N− bond rotation. We calculate a cis → trans barrier height of 33 kcal/mol for S_0 rehybridization, compared to a 48 kcal/mol barrier for S_0 ring rotation. When comparing the calculated results for isomerization on the S_0 and S_1 surfaces, a relatively

SCHEME 2: (top) Resonance Structures for 4,4′-Diaminoazobenzene;[a] (bottom) Resonance Structures for a 4,4′-Diamidoazobenzene[b]

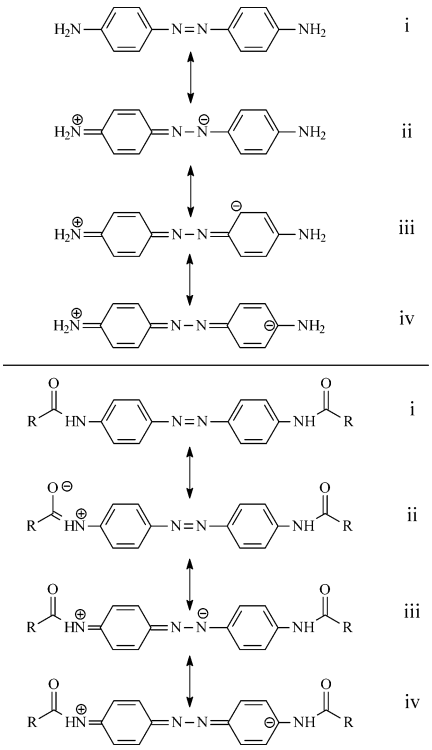

[a] All structures are expected to contribute because of the presence of the electron-donating amine groups. [b]Structures iii and iv are expected to not contribute significantly because of the electron-withdrawing character of the amide groups.

small S_1 barrier is indicated for rehybridization (~12 kcal/mol), and the S_1 surface is calculated to be barrierless for ring rotation. While it is tempting to use this information to infer the dominance of N═N rotation as the dominant isomerization coordinate in the S_1, we do not feel justified in making this conclusion because an almost barrierless isomerization pathway can be traced out on either surface, provided the ring rotation coordinate has sufficient time to locate the minimum on the S_1 surface prior to relaxation back to the S_0 surface. These calculated results should be taken as an indication of the substantially more facile nature of isomerization on the S_1 surface than is possible on the S_0 surface for azobenzene.

Conclusions

Our investigation of a family of symmetrically disubstituted azobenzenes has shown that significant control over the linear optical and isomerization properties of these molecules can be exerted synthetically. The experimental spectra point to diaminoazobenzene being different than diamidoazobenzene and azobenzene, both in terms of ground-state isomerization barrier and branching ratio. We find that the experimental S_0 barrier to back-isomerization is correlated with the $S_1 \leftarrow S_0$ transition cross section, and we attribute this relationship to the strength of vibronic contributions to the isomerization transition state. These experimental results combined with calculated isomerization surfaces indicate that the ground-state isomerization of azobenzenes proceeds by rehybridization of one of the azo nitrogens rather than by rotation about the −N═N− bond. These calculations provide no analogous clear indication of the dominant isomerization process on the S_1 surface. We anticipate, on the basis of these results, that we can, through synthetic means, demonstrate even greater control over the isomerization barrier height for azobenzenes, and this control will be of use in controlling the dynamics of this family of molecules in restricted environments.

Acknowledgment. We are grateful to the National Science Foundation for support of this work through Grant 0090864.

References and Notes

(1) Saremi, F.; Tieke, B. *Adv. Mater.* **1998**, *10*, 388.
(2) Wang, C.; Fei, H.; Xia, J.; Yang, Y.; Wei, Z.; Yang, Q.; Sun, G. *Appl. Phys. B: Laser Opt.* **1999**, *68*, 1117.
(3) Howe, L. A.; Jaycox, G. D. *J. Polym. Sci., Part A: Polym. Chem.* **1998**, *36*, 2827.
(4) Yoshii, K.; Machida, S.; Horie, K. *J. Polym. Sci., Part B: Polym. Phys.* **2000**, *38*, 3098.
(5) Aoshima, Y.; Egami, C.; Kawata, Y.; Sugihara, O.; Tsuchimori, M.; Watanabe, O.; Fujimara, H.; Okamoto, N. *Polym. Adv. Technol.* **2000**, *11*, 575.
(6) Zilker, S. J.; Bieringer, T.; Haarer, D.; Stein, R. S.; van Egmond, J. W.; Kostromine, S. G. *Adv. Mater.* **1998**, *10*, 855.
(7) Eichler, H. J.; Orlic, S.; Schulz, R.; Rubner, J. *Opt. Lett.* **2001**, *26*, 581.
(8) Hagen, R.; Bieringer, T. *Adv. Mater.* **2001**, *13*, 1805.
(9) Pedersen, T. G.; Johansen, P. M.; Pedersen, H. C. *J. Opt. A: Pure Appl. Opt.* **2000**, *2*, 272.
(10) Patane, S.; Arena, A.; Allegrini, M.; Andreozzi, L.; Faetti, M.; Giordano, M. *Opt. Commun.* **2002**, *210*, 37.
(11) Astrand, P.-O.; Ramanujam, P. S.; Hvilsted, S.; Bak, K. L.; Suauer, S. P. A. *J. Am. Chem. Soc.* **2000**, *122*, 3482.
(12) Tamada, K.; Akiyama, H.; Wei, T.-X.; Kim, S.-A. *Langmuir* **2003**, *19*, in press.
(13) Misra, G. S. *Introductory Polymer Chemistry*; Wiley Eastern Limited: New Delhi, India, 1993.
(14) Fujino, T.; Arzhantsev, S. Y.; Tahara, T. *J. Phys. Chem. A* **2001**, *105*, 8123.
(15) Saito, T.; Kobayashi, T. *J. Phys. Chem. A* **2002**, *106*, 9436.
(16) Lednev, I. K.; Ye, T.-Q.; Matousek, P.; Towrie, M.; Foggi, P.; Neuwahl, F. V. R.; Umapathy, S.; Hester, R. E.; Moore, J. N. *Chem. Phys. Lett.* **1998**, *290*, 68.
(17) Lednev, I. K.; Ye, T. Q.; Abbott, L. C.; Hester, R. E.; Moore, J. N. *J. Phys. Chem. A* **1998**, *102*, 9161.
(18) Zimmerman, G.; Chow, L. Y.; Paik, U. J. *J. Am. Chem. Soc.* **1958**, *80*, 3528.
(19) Rulliere, C. *Chem. Phys. Lett.* **1976**, *43*, 303.
(20) Andersson, J. A. *J. Photochem.* **1983**, *22*, 245.
(21) These macros are available from the corresponding author upon request.